Two dimension simulation of chest wall hyperthermia

Songul Barlaz Us[1*], Hafiz Z. Alisoy[2], B.Baykant Alagoz[2]
[1]*Department of Radiation Oncology, Inonu University School of The Medicine, Malatya, Turkey*
[2]*Department of Electric-Electronic Engineering, Inonu University Faculty of Engineering, Malatya, Turkey*

Abstract

One of the cancer treatment methods is hyperthermia. In this study, by using cross section computer tomography (CSCT) of chest wall which the patient has been treated with radiotherapy for the single-source was placed into (internally) and out (externally) of the chest wall. SAR (Spesific Absorbtion Rate) distribution on the chest wall is numerically calculated by using finite difference time domain (FDTD) based electromagnetic wave propagation simulation.

Keywords: Hyperhermia; Spesific absorbtion rate; Finite difference time domain; Simulation; Cross section computer tomograpy.

1.Introduction

Hyperthermia is a treatment method which makes the treatment of tumors possible by increasing the temperature and is used with the combination of the radiation therapy or chemotherapy [1-3]. Not only is the hyperthermia used for the breast cancer, bone metastasis, sarcoma, melanoma, carcinoma, lung, stomach, pancreas, gall bladder, kidney, neck and brain tumors, breast, cervical, and others cancer types alone, but it can also be used for rectum, prostate, bladder cancer, lung, stomach, pancreas head-neck, liver and superficial tumors as a treatment to help [4-6]. Since the temperature is raised from 37˚C to 41˚C–46˚C systematically in hyperthermia, cancer cells are damaged [7]. Damage to the tissue is the same although heating methods used are different in hyperthermia techniques. For heating, externally applied microwaves, interstitial microwave heating that using antennas implanted, ultrasound waves, radiofrequency and lasers are used [1, 8, 9].

Different source types are used and source design studies are still to be continued in hyperthermia. In his study, Sullivan [10] used prototype source design for hyperthermia. Bai et al. [11] made circular-shaped and slotted sources to improve traditional Vivaldi antenna at low frequency performance. Peng et al. [12] prepared single-pole antenna model and analiysed in an ultra-wide band.

Sun et al. [13] developed criyo-heating probe for breast tumors in theory. Rapoport et. al. [14] placed micro bubbles in ovarian, breast, and pancreatic cancerous tumors, emitting therapeutic ultrasound waves.

[*]Corresponding author: Tel: +90-5058955284; fax: +90-4223410660
E-mail address: songul.barlaz@inonu.edu.tr (S.Barlaz Us).

Aitkenhead et al. [9] made planar ultrasound transducer design for the hyperthermia of the solid tumours located in the deep stage of the body. Keangin et al. [15] sent the single-and double-hole antenna type which produces micro wave into the tissue in the liver model. Vogl et al. [16] settled an electrode emitting microwave and radiofrequency laser fort the thermal ablation of lung cancer tissue.

Based on Pennes bio-heat equation in the hyperthermia, the temperature distribution of tissues have been examined [17]. Many methods have been used for the numerical analysis of the distribution of electromagnetic waves in a tissue. Miyazaki et al. [18], Simicevic et al. [19] and Tofighi [20] have used FDTD in their studies. Costen et al. [21] compared finite difference time domain method by taking Huygens techniqueas reference. Drezek et al. [22] combined FDTD with pulse reply technique in order to calculate the light spreading feature of the biological tissues.

In this study, FDTD has been developed in the MATLAB version 7.0.1. for the numerical analysis of the electromagnetic microwave. A point source of 6.8 GHz sinusoidal microwave has been used in the FDTD simulation. The point source has been placed into and out of the chest wall on the CSCT. Two dimentional SAR distributions obtained from there have been evaluated.

2. Materials and methods

2.1. Parameterization of anatomical tissues for FDTD simulation

Basically, the dielectric constants of tissues must be known in order to analyse the effects of electromagnetic waves on the biological tissues. Gabriel et al. [23] summarized and presented the dielectric properties of the biological tissues graphically for the last 50 years. Many organs and tissues in different frequency ranges for the conductivity and dielectric constant have been presented and a a fundamental literature base for the further studies have been obtained.

In the study, 6.8 GHz frequency sinusoidal wave has been used. Medium parameters at the frequency value of 6.8 GHz are shown in table 1 (conductivity- σ, static dielectric permittivity - ε_s and optical dielectric permittivity - ε_∞, relaxation time- τ_0) [21].

Table 1. Parameters of biological tissues, at the frequency value of 6.8 GHz [21]

Medium	σ(S/m)	ε_∞ (F/m)	ε_s (F/m)	τ_0 (ps)
Air	$1x10^{-14}$	1	1	0
Skin	0.49	30	79	62
Fat	$3x10^{-2}$	3.5	6.2	39
Muscle	0.7	42	100	49
Lung	0.3	14	36	48
Bone	$1.9x10^{-2}$	4.2	9.5	77
Heart Muscle	0.58	48	280	206

By regarding these four parameters in the Debye model, the measurable dielectric permittivity used in electrical modeling of the chest wall has been calculated through the following formula [24],

$$\varepsilon = \varepsilon_\infty + \frac{\varepsilon_0 - \varepsilon_\infty}{\left[1 + (i\omega\tau_0)\right]} - j\frac{\sigma}{\varepsilon_0\omega} \qquad (1)$$

Here, $\varepsilon_0 = 8.85x10^{-12}$ F/m is dielectric permittivity of the free space, $\omega = 2\pi f$ is angular frequency and f is the linear frequency of the wave.

SAR, which depends on the energy of the electromagnetic wave, effective conductivity and mass density, is calculated through the following formula [25-28],

$$SAR = \sigma_{eff} \frac{\left|\vec{E}\right|^2}{2\rho} \quad (2)$$

In the formula, ρ is the tissue density and σ_{eff} is the effective conductivity. The effective conductivity can be calculated throughthe following formula [25].

$$\sigma_{eff} = \sigma - \omega\varepsilon_0 imag\left\{\frac{\varepsilon_s - \varepsilon_\infty}{1 + j\omega\tau_0}\right\} \quad (3)$$

By taking the value of tissue density and explanations of the study of Chapla et al. [29] into consideration, the calculated dielectric permittivity and value of the effective conductivity are being shown in the table 2.

Table 2. Relative permittivity, effective conductivity and tissue density values of biological tissues

Medium	ε_r	σ_{eff} (S/m)	ρ (kg / m^3)
Air	1	1x10^{-14}	1.3
Skin	36.11	6.61	1118
Fat	4.21	0.48	999
Muscle	52.77	9.23	1119
Lung	18.23	3.58	1.3 (equivalent air)
Bone	4.65	0.58	2500*
Heart Muscle	50.96	10.42	1119 (equivalent muscle)

*Average value of different bones in the study [29]

2.2. FDTD based numerical simulation

Real wave propagation mediums exhibit attenuation effects, which is mainly characterized by a loss term, namely conductivity. In order to model the EM propagation in the lossy mediums, Maxwell equations have been written as follows [30]:

$$\varepsilon \frac{\partial \vec{E}}{\partial t} = \nabla x \vec{H} - \sigma \vec{E} \quad (4)$$

$$\frac{\partial \vec{H}}{\partial t} = -\frac{1}{\mu_0} \nabla x \vec{E} \quad (5)$$

One can reorganize time dependence of electrical field in the equation (5) as,

$$\frac{\partial \vec{E}}{\partial t} = \frac{1}{\varepsilon_r \varepsilon_0} \nabla x \vec{H} - \frac{\sigma}{\varepsilon_r \varepsilon_0} \vec{E} \quad (6)$$

If $\tilde{E} = \vec{E}\sqrt{\frac{\varepsilon_0}{\mu_0}}$ normalization is made for the electric field vector and the wave propagation in transverse magnetic (TM) mode is written for a two-dimensional (2D) spatial domain, as

$$\frac{\partial \tilde{E}_z(t)}{\partial t} = \frac{1}{\varepsilon_r \sqrt{\varepsilon_0 \mu_0}} \left(\frac{\partial H_y(t)}{\partial x} - \frac{\partial H_x(t)}{\partial y}\right) - \frac{\sigma}{\varepsilon_r \varepsilon_0} \tilde{E}_z(t) \quad (7)$$

$$\frac{\partial H_x(t)}{\partial t} = -\frac{1}{\sqrt{\varepsilon_0 \mu_0}} \frac{\partial \tilde{E}_z(t)}{\partial y} \tag{8}$$

$$\frac{\partial H_y(t)}{\partial t} = \frac{1}{\sqrt{\varepsilon_0 \mu_0}} \frac{\partial \tilde{E}_z(t)}{\partial x} \tag{9}$$

When finite differences linearization is applied to the derivatives terms in the equations (7), (8) and (9), the following finite difference equations are obtained:

$$H_x^{n+1/2}(i,j) = H_x^{n-1/2}(i,j) - \frac{\Delta t}{\sqrt{\varepsilon_0 \mu_0}} \frac{\tilde{E}_z^n(i,j+1) - \tilde{E}_z^n(i,j)}{\Delta y} \tag{10}$$

$$H_y^{n+1/2}(i,j) = H_y^{n-1/2}(i,j) + \frac{\Delta t}{\sqrt{\varepsilon_0 \mu_0}} \frac{\tilde{E}_z^n(i+1,j) - \tilde{E}_z^n(i,j)}{\Delta x} \tag{11}$$

$$\begin{aligned} \tilde{E}_z^{n+1}(i,j) = \tilde{E}_z^n(i,j) - \frac{\Delta t}{\varepsilon_r \sqrt{\varepsilon_0 \mu_0}} \Big(& \frac{H_x^{n+1/2}(i,j) - H_x^{n+1/2}(i,j-1)}{\Delta y} \\ & - \frac{H_y^{n+1/2}(i,j) - H_y^{n+1/2}(i-1,j)}{\Delta x} \Big) - \frac{\sigma \Delta t}{\varepsilon_r \varepsilon_0} \frac{\tilde{E}_z^{n+1}(i,j) + \tilde{E}_z^n(i,j)}{2} \end{aligned} \tag{12}$$

The parameters Δx and Δy are horizontal and vertical unit distances for 2D spatial domain. A square solution point grid on this 2D plane has been defined in the simulation by setting $\Delta x = \Delta y$. The parameter Δt is a unit time increment for the solutions in temporal domain. In order to obtain a stable EM wave propagation in the spatio-temporal domain, the Courant stability criteria, expressed as $\Delta t \le \frac{\Delta x}{\sqrt{2} \cdot c}$, has been considered to determine an appropriate value of Δt. Here, $c = 1/\sqrt{\varepsilon_0 \mu_0}$ stands for the velocity of electromagnetic wave in a vacuum. By taking the unit time increment as $\Delta t = \frac{\Delta x}{\sqrt{2} \cdot c}$ for a stable wave propagation on a 2D square solution grid into account, the equation (12) can be rearranged as follows [26, 31]:

$$\begin{aligned} \tilde{E}_z^{n+1}(i,j) = & \frac{(1-\alpha)}{(1+\alpha)} \tilde{E}_z^n(i,j) - \frac{1/\sqrt{2}}{\varepsilon_r (1+\alpha)} \cdot \\ & \cdot \left[H_x^{n+1/2}(i,j) - H_x^{n+1/2}(i,j-1) + H_y^{n+1/2}(i-1,j) - H_y^{n+1/2}(i,j) \right] \end{aligned} \tag{13}$$

where in the expression (13), $\alpha = \frac{\Delta t . \sigma}{2 \varepsilon_r \varepsilon_0}$.

The finite difference equations given by equations (10), (11) and (13) have been used to simulate microwave propagation in a lossy inhomogeneous media that has been modeled by the electrical parameters, the dielectric permittivity and the conductivity.

In this study, before anything else, coloring has been made in the CSCT to indicate the color coding of environment that will be analyzed. Each tissue has been painted with different colors on the CSCT. Skin, muscle, bone, heart muscle, lung and spinal cord have been coded as turquoise, red, white, pink, gren and yellow, respectively. Source color has been defined as blue and its parameters have been taken as equivalent to the parameters of the air. Numerical simulation has been made in two steps: In the first step, by using the electrical parameters in table 1, in an environment defined by a CSCT, the microwave

propagation of FDTD simulation code has been written. In the second step, on the other hand, based on the formula (2), the SAR distributions have been calculated by using the parameters presented in table 2.

3. Results and discussion

In this study, performed on the CSCT, point sinuzoidal source has been placed externally and internally in the chest wall tissue. CSCT used and the modellings are showed in the figure 1.

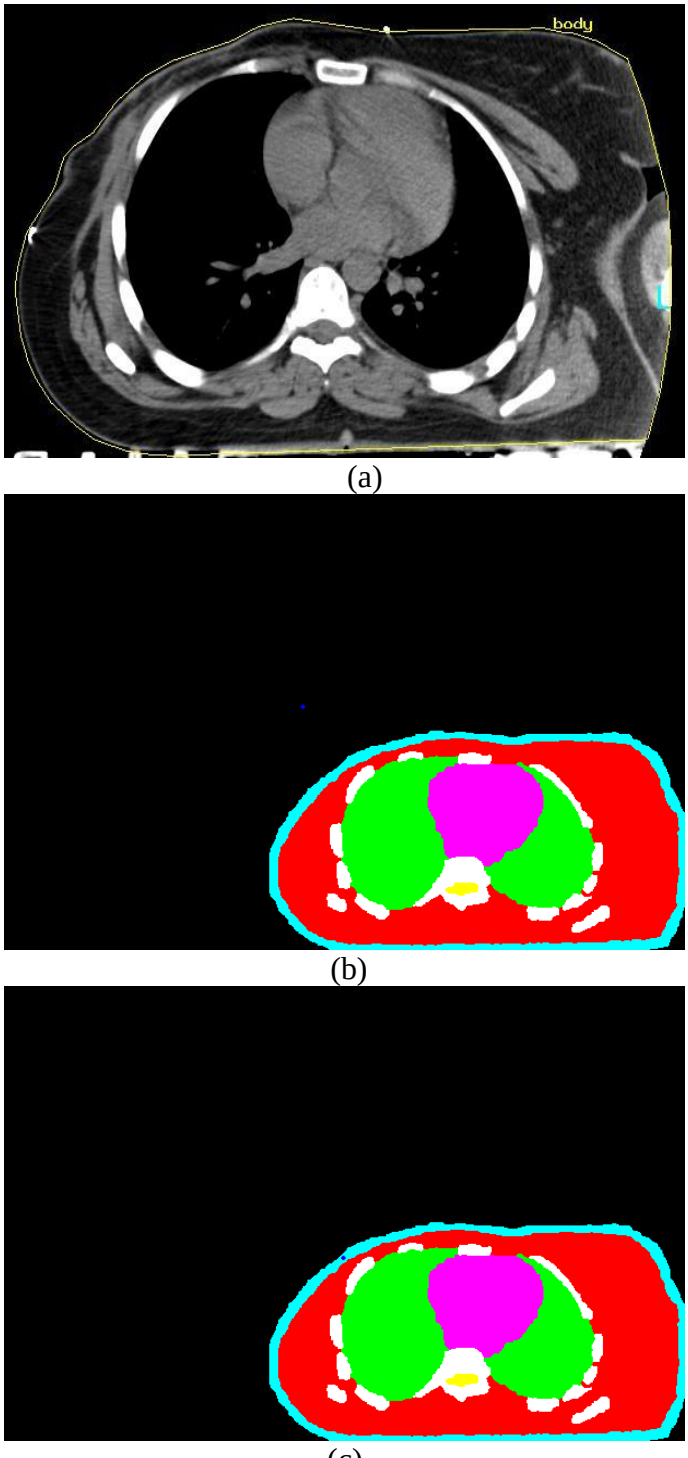

(a)

(b)

(c)

Fig 1.(a) CSCT of the chest wall

(b) Simulation model placed externally
(c) Simulation model placed internally

Simulation scale has been set by taking the actual size of the CSCT into consideration and simulation has been completed in 400 steps. As a result of the simulation, the sources that have been placed internally and externally and linear and painterly distributions of SAR are shown in figure 2 and figure 3. Distributions are given on a logarithmic scale in order to see the significant changes among the tissues. Intermediate values, which do not appear in the line distributions, are seen in pictorial distributions.

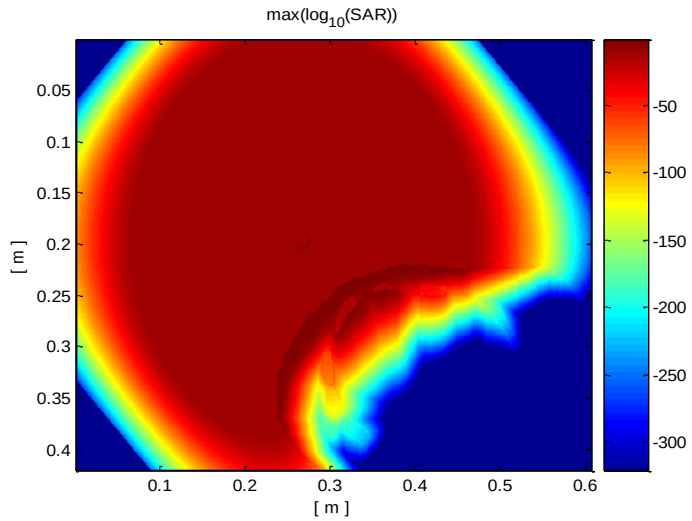

(a)

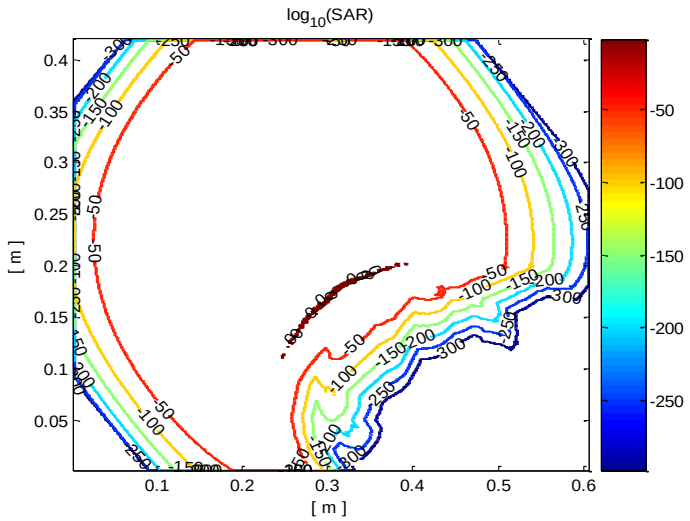

(b)

Fig 2. The SAR distribution in case of using external source
(a) Painterly disturibution
(b) Linear disturibution

When the source is placed outside of the skin, the wave that comes to the skin begins to be attenuated as it reaches to an environment which has a lower conductivity than air. Although SAR is increased suddenly on muscle-fat interface in Sullivan [26]'s study for radiofrequency waves, as skin, fat and muscle are very thin layers, these tissues

interface are identical to the SAR. The main difference occurs because of the bone tissue. Due to the intensity of the bone tissues and difference of the conductivity/intensity rate, the wave is reflected from this region. Thus, less absorption occurs in the bones; however, a very high absorption occurs around the bones. Likewise, in the Moros et. al. [5]'s study, sharp power absorption has occured on the soft tissue-bone interface for ultrasound waves. For the chest wall region, as it can be seen from the SAR distributions, the electromagnetic wave energy absorption is quite homogeneous. The fact that wave which transmits to the bone tissue is a weak causes the critical organs on backbone such as lungs and heart to be protected. It is a desired result for the cancer treatment that critical tissues and organs take minimum absorption in the treatment of the chest wall.

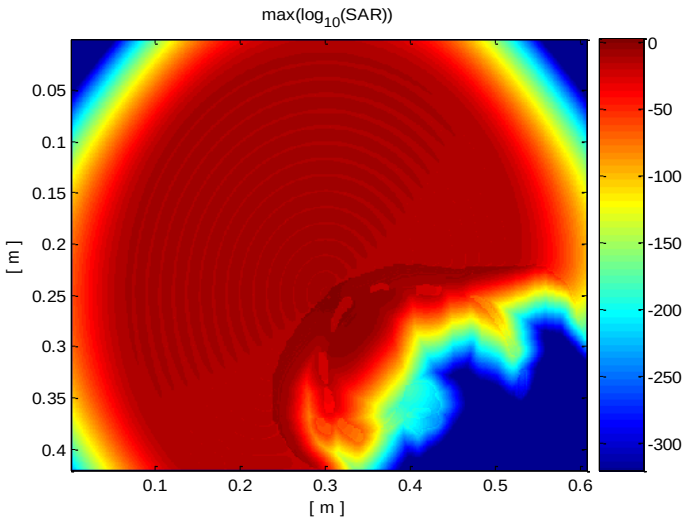

(a)

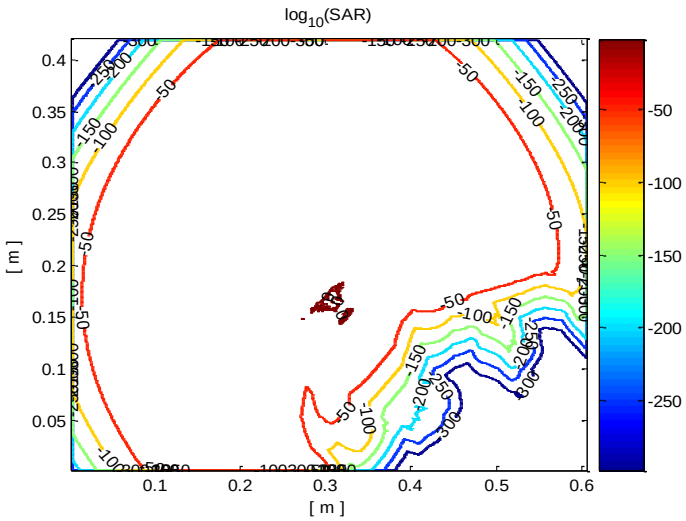

(b)

Fig 3. The SAR distribution in case of using internal resources

(a) Painterly disturibution

(b) Linear disturibution

When the source is inserted into the chest wall on the CSCT, the interactions are similar to the case in which the source is placed outside. The source of the placed in the chest wall causes an increased absorption at a certain distance from the source location due to the strong reflections around the high density bone tissue. This condition is caused by

the collection of the reflected waves depending on the point source. As it can be seen in the distribution of pictorial SAR, absorption occurs in the interior of the chest wall, even at the bottom of the ribcage. The wave force of internal source is higher than the wave force of external source. However, when the source was placed out of the chest wall, a more homogeneous dispersion in a larger area was obtained. When the source was placed in the chest wall, the wave absorbtion is less homogeneous and absorbtion is focused on a small region. Thus, a homogeneous distribution was not seen on the chest wall.

4. Conclusıon

In this study, chest wall hyperthermia was simulated by using a microwave point source. SAR distributions were obtained and compared as a result of the the position of the point source for two cases, that is, the point source is placed inside or outside the chest wall. With regard to the two-dimensional SAR distribution resulted from CSCT, it was deduced that: i) a homogeneous dispersion was obtained in a small region for the case in which the point source was placed inside the chest wall, ii) however, relatively a more homogeneous SAR distribution in a larger region was obtained for the case in which the point source was placed outside the chest wall, iii) in both applications, the critical organs such as lung and heart behind the bone tissue, were not influenced considerably from the emission of the point source. However, in the case in wihch the point source was placed into the chest wall, the absorption was increased as a result of the reflected waves occurred due to the high density bone structure. The increase in the absorbtion in the inner regions is higher in comparison with the case in which the external source is used; therefore, it is supposed that it is more proper to use external point source chest wall in hyperthermia applications.

Symbols

σ	conductivity (S/m)
σ_{eff}	effective conductivity (S/m)
ε_s	static dielectric permittivity
ε_∞	optical dielectric permittivity
τ_0	relaxation time (s)
ω	angular frequency (rd/s)
f	linear frequency (Hz)
ρ	density (kg/m^3)
E	electric field (V/m)
H	magnetic field (A/m)
Δt	unit time (s)
Δx, Δy	unit distance (m)
c	light velocity ($3x10^8$ m/s)

References

[1] Singh VR. "Ultrasound hyperthermia control system for deep-seated tumours: exvivo study of excised tumours, modeling of thermal profile and future nanoengineering aspects," *IRBM,* 2008;29, pp. 326–36.

[2] Chichel A, Skowronek J, Kubaszewska M, et al. "Hyperthermia – description of a method and a review of clinical appl.," *Rep Pract Oncol Radiother,* 2007;vol. 12, pp. 267-75.

[3] Zagar TM, Higgins KA, Miles EF, et al. "Durable palliation of breast cancer chest wall recurrence with radiation therapy, hyperthermia, and chemotherapy," *Radiotherapy and Oncology,* 2010; vol 97, pp. 535–40.

[4] Mahjoob S, Vafai K, "Analytical characterization of heat transport through biological media incorporating hyperthermia treatment," *International J Heat and Mass Transfer*, 2009;vol. 52, pp. 1608–18.

[5] Moros EG, Fan X, Straube WL, "Ultrasound power deposıtıon model for the chest wall," *Ultrasound in Med. & Biol*, 1999;vol. 25**,** pp. 1275–87,.

[6] Lu BY, Yang RS, Lin WL, et al. "Theoretical study of convergent ultrasound hyperthermia for treating bone tumors," *Medical Eng & Physics*, 2000;vol. 22, pp. 253–63.

[7] Gupta PK, Singh J, Rai KN, "Numerical simulation for heat transfer in tissues during thermal therapy," *Journal Of Thermal Biology*, 2010;vol. 35, pp. 295–301.

[8] Converse M, Bond EJ, Van Veen BD, et al. "A computational study of ultra-wideband versus narrowband microwave hyperthermia for breast cancer treatment," *IEEE Transactıons On Mıcrowave Theory And Techniques,* 2006;vol. 54, pp. 2169-80,.

[9] Aitkenhead AH, Mills JA, Wilson AJ, "The design and characterization of an ultrasound phased array suitable for deep tıssue hyperthermia," *Ultrasound in Med. & Bio*, 2008; vol. 34, pp. 1793– 07.

[10] Sullivan D. "Three-dimensional computer simulation in deep regional hyperthermia using the finite-difference time-domain method," *IEEE Transactıons On Mıcrowave Theory And Techniques,* 1990;vol. 38, pp. 204-21.

[11] Bai J, Shi S, Prather W. "Modified compact antipodal vivaldi antenna for 4–50-GHz UWB application," *IEEE Transactıons On Microwave Theory And Techniques*, 2011;vol. 59, pp. 1051-7.

[12] Peng L, Ruan CL. "UWB band-notched monopole antenna design using electromagnetic-bandgap structures," *IEEE Transactions on Microwave Theory And Techniques*, 2011;vol. 59, pp. 1074-81.

[13] Sun J, Zhang A, Xu LX. "Evaluation of alternate cooling and heating for tumor treatment," *International J Heat And Mass Transfer*, 2008 vol. 51, pp. 5478–85.

[14] Rapoport NY, Kennedy AM, Shea JE, et al. "Controlled and targeted tumor chemotherapy by ultrasound-activated nanoemulsions/microbubbles," *J Controlled Release*, 2009;vol. 138, pp. 268–76.

[15] Keangin P, Rattanadecho P, Wessapan T, "An analysis of heat transfer in liver tissue during microwave ablation using single and double slot antenna," *International Communications in Heat and Mass Transfer***,** *ICHMT-02354*, 10, 2011.

[16] Vogl TJ, Naguib NNN, Lehnert T, et al. "Radiofrequency, microwave and laser ablation of pulmonary neoplasms: Clinical studies and technical considerations—Review article," *European J Radiology*, 2011;vol. 77, pp. 346–57.

[17] Pennes HH."Analysis of tissue and arterial blood temperatures in the resting human forearm," *Journal of Applied Physiology*, 1948;vol. 1, pp. 93-22.

[18] Miyazaki Y, Kouno K. " FDTD analysis of spatial filtering of scattered waves for optical ct of medical diagnosis," *Progress In Electromagnetics Research Symposium*, pp. 2009;1567-72.

[19] Simicevic N, Hayniye DT."FDTD simulation of exposure of biological material to electromagnetic nanopulses," *Phys. Med. Biol*, 2005;vol. 50, pp. 347–60.

[20] Tofighi MR. "FDTD modeling of biological tissues cole–cole dispersion for 0.5–30 GHz using relaxation time distribution samples—novel and improved implementations," IEEE *Transactıons On Mıcrowave Theory And Techniques,* 2009; vol. 57, pp. 2588-96,.

[21] Costen F, Bérenger JP. "Extension of the FDTD huygens subgridding to frequency dependent media," *Ann. Telecommun DOI 10.1007/s12243-009-0131-0*. 2009.
[22] Drezek R, Dunn A, Kortum RR. "A pulsed finite-difference time-domain (FDTD) method for calculating light scattering from biological cells over broad wavelength ranges," *Optıcs Express,* 2000;vol. 6, pp. 147-57.
[23] Gabriel C, Gabriely S, Corthout E. "The dielectric properties of biological tissues: I. Literature survey," *Phys. Med. Biol*, 1996;vol. 41, pp. 2231–49.
[24] Kao KC. *Dielectric phenomena in solids: with emphasis on physical concepts of electronic processes*, Elsevier Academic Pres, 2004.
[25] Sullivan DM. "A frequency-dependent FDTD method for biological applications," *IEEE Transactions on Mıcrowave Theory and Techniques,* 1992; vol. 40, pp. 532-9.
[26] Bri S, Kassimi S, Habibi M, et al. "Specific absorption rate (SAR) distribution in the human head at global system mobil (GSM) frequencies," *European J Scientific Research* **,** 2011;vol. 49 , pp. 590- 00.
[27] Gangwar RK, Singh SP, Kumar D. "SAR distribution in a bio-medium in close proximity with rectangular dielectric resonator antenna," *Progress In Electromagnetics Research B,* 2011;vol. 31, pp. 157-73.
[28] Wasife EK. "Power density and SAR in multi-layered life tissue at global system mobile (GSM) frequencies," *J Electromagnetic Analysis and Applications,* 2011;vol. 3, pp. 328-32.
[29] Chapla ME, Nowacek DP, Rommel SA, et al. "CT scans and 3D freconstructions of Florida manatee (Trichechus Manatus Latirostris) heads and ear bones," *Hearing Research,* 2007;vol. 228, pp. 123–35.
[30] Umashankar K, Taflove A. *Computational Electromagnetics*. Artech House, Boston, USA, 1993.
[31] Taflove A. *Computational Electrodynamics: The Finite Difference Time Domain Method*. Artech House, Boston, USA, 1995.